City Research Online

City, University of London Institutional Repository

Citation: Kappos, A. J., Papadopoulos, I. and Tokatlidis, A. (2014). Design of a Seismically Isolated Railway Viaduct over Axios River in Northern Greece. Paper presented at the Second International Conference on Railway Technology: Research, Development and Maintenance, 8-11 April 2014, Ajaccio, Corsica.

This is the accepted version of the paper.

This version of the publication may differ from the final published version.

Permanent repository link: https://openaccess.city.ac.uk/id/eprint/16035/

Link to published version:

Copyright: City Research Online aims to make research outputs of City, University of London available to a wider audience. Copyright and Moral Rights remain with the author(s) and/or copyright holders. URLs from City Research Online may be freely distributed and linked to.

Reuse: Copies of full items can be used for personal research or study, educational, or not-for-profit purposes without prior permission or charge. Provided that the authors, title and full bibliographic details are credited, a hyperlink and/or URL is given for the original metadata page and the content is not changed in any way.

City Research Online: http://openaccess.city.ac.uk/ publications@city.ac.uk

C123 Kappos, A. J., Papadopoulos I., and Tokatlidis A. “Design of a Seismically Isolated Railway Viaduct over Axios River in Northern Greece”, Railways 2014: The Second Intern. Conference on Railway Technology, Ajaccio, Corsica, 8-11 Apr. 2014, Civil-Comp Press, paper no. 80

Abstract

The paper presents the salient features of the design of the Railway viaduct over Axios River on the new high-speed double railway line, which is the longest (800m) railway bridge in Greece constructed using the travelling gantry method. Located in a high seismic hazard area, the viaduct is provided with an isolation system aiming to reduce the structural response to seismic loading, a solution that presents several challenges in the case of railway bridges and cannot be implemented solely on the basis of existing codes. Lead-rubber bearings are provided at each pier to deck connection and system damping is further increased through fluid viscous dampers at each abutment. To verify the performance of the isolation system, analysis for seismic actions is conducted in three discrete stages of increasing complexity. Seismic forces and displacements are found to be within acceptable limits and serviceability requirements are also met. Conclusions are drawn regarding the feasibility of using passive systems in railway bridges in seismic areas.

Keywords: Railway bridges, Seismic Isolation, Nonlinear analysis, Eurocode 8-2.

1 Introduction

The design of railway bridges presents a number of challenges when these are located in high seismic hazard areas. In particular when seismic isolation (reduction in seismic demand through lengthening the natural periods and increasing the energy dissipation capacity) is a viable solution, several issues have to be addressed, not least of which is the accommodation of the seismic displacements that should not hinder the proper function of the railway bridge. Moreover, when dampers are used to increase the energy dissipation capacity, verification of the isolated structure has to be carried out using advanced analysis techniques (nonlinear response-history analysis for properly selected and scaled ground motions). The paper presents the salient features of the design of a recently constructed railway viaduct, with special emphasis on seismic aspects, and identifies instances where the application of current codes is far from straightforward, suggesting specific solutions to the problems encountered, in a practical design context.

1.1 Project Information

The new High-Speed Railway Line in Northern Greece, from Thessaloniki to Edomeni, crosses the Valley of Axios River on an 800 m long viaduct (bridge T12) at a maximum height of 40 m above ground level. The horizontal alignment is partly curved in plan with a 270 m long straight section, followed by a 180 m long clothoid transition to a curve with a 2200 m radius. Longitudinally the gradient is 1.6%, while at the abutments the slope gradient varies from 30% to 50%. For a design speed V≤200km/h the required total deck width is 13.90 m. The bridge superstructure is a continuous 18-span prestressed concrete box girder of constant depth 3.60 m (see Figure 1) with expansion joints only at the abutments. Typical span length is 45 m while end spans are 40 m long (40+16×45+40=800m). Bridge piers are circular hollow columns with outside diameter 4.50 m, wall thickness 500 mm, and clear heights between 15.0 and 36.0m. The interior of the structure (deck, piers, abutments) is accessible for inspection. Considering all of the above features (span, height, section, total length), the bridge deck was erected using the travelling gantry method (suited for viaducts with spans in the range of 30 to 60 m). Construction of the project was completed at the end of 2009 with a total cost of around 12 million Euros.

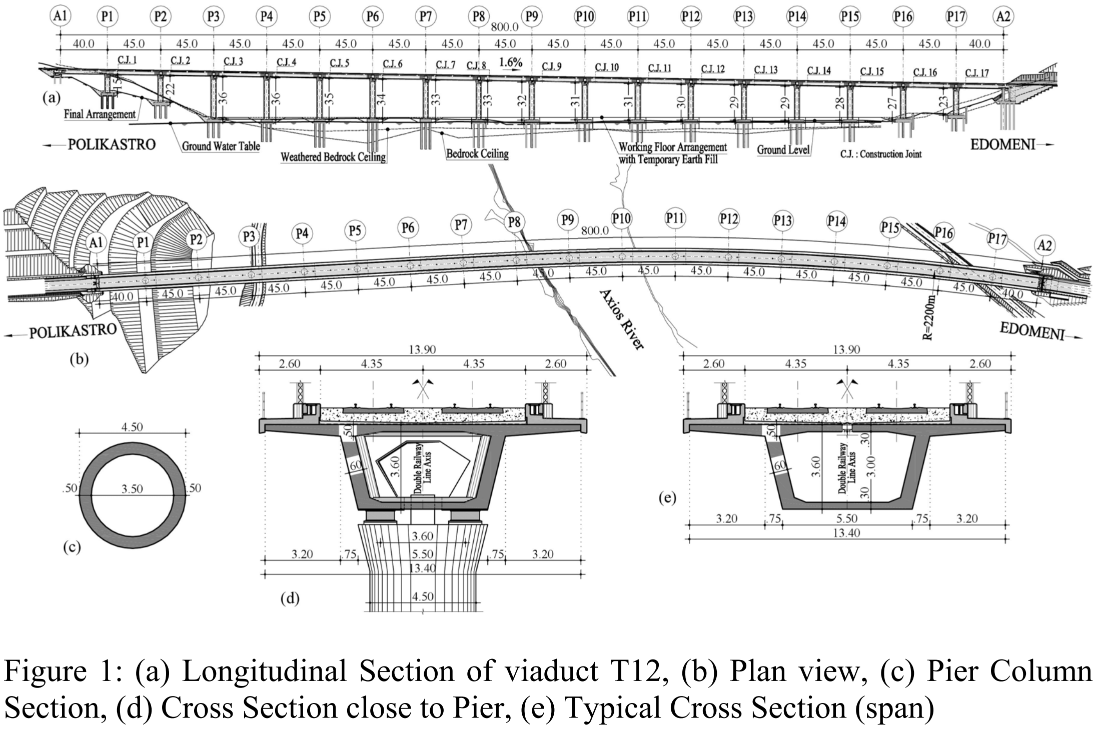
A1
P1
P2
P3
P4
P5
P6
P7
P8
P9
P10
P11
P12
P13
P14
P15
P16
P17
A2
800.0
40.0
45.0
1.6%
C.J. 1
C.J. 17
(a)
Final Arrangement
POLIKASTRO
Ground Water Table
Weathered Bedrock Ceiling
Bedrock Ceiling
Working Floor Arrangement with Temporary Earth Fill
Ground Level
C.J. : Construction Joint
EDOMENI
(b)
Axios River
R=2200m
(c)
4.50
.50
3.50
13.90
2.60
4.35
3.60
Double Railway Line Axis
3.20
.75
5.50
13.40
(d)
(e)
3.00

Figure 1: (a) Longitudinal Section of viaduct T12, (b) Plan view, (c) Pier Column Section, (d) Cross Section close to Pier, (e) Typical Cross Section (span)

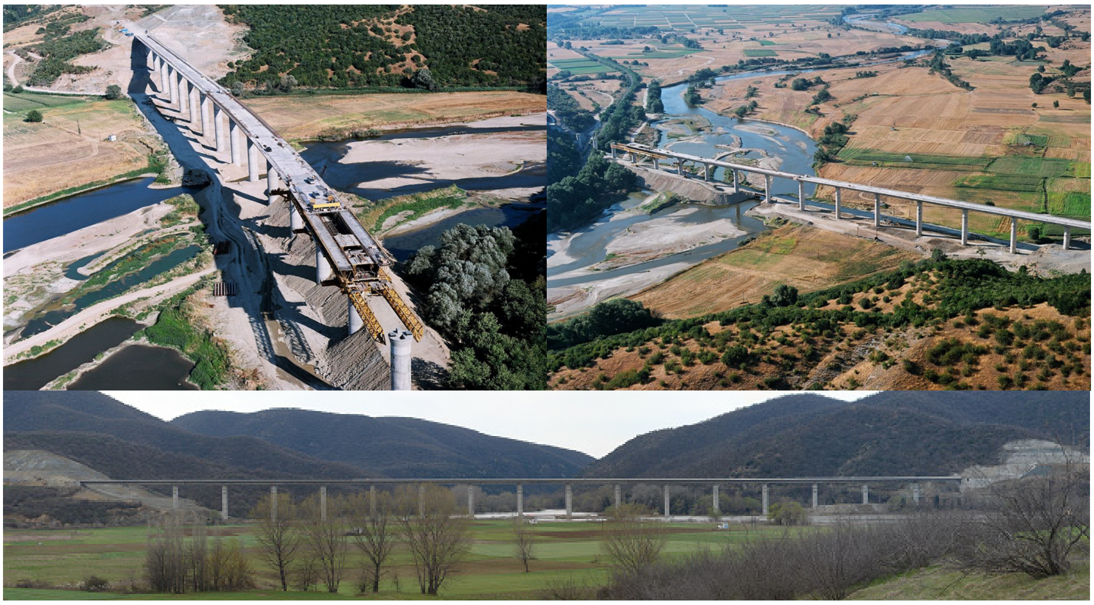

Figure 2: Various aspects of the T12 viaduct

2 Ground Conditions and Design Seismic Action

An extensive geotechnical investigation (including a total of 19 boreholes) was carried out to identify ground conditions in the bridge site. Bedrock is found at a shallow depth and is generally of medium quality, with some extended shear zones and a weathered layer at the top. Alluvial deposits with a medium to loose density are found in the area of the river bed, which in the future may possibly displace horizontally and therefore broaden. Scour and erosion in the river bed is possible up to a depth of 7 to 8 m. A debris layer is found in the area of the west abutment (Pier P17 and A2, see Fig. 1a). Creep in the embankment slope of the east abutment (A1) which was identified through inclinometers at an earlier stage, was dealt with an extended excavation to reduce the slope angle and the mass of the embankment, and also by adding another span (A1-P1).

Taking into account the above data, and in order to safely transfer the high loads of the supporting members to the ground, use of deep foundation was selected. Piers rest on pile-supported cap footings with pile lengths between 11.0 and 25.0 m and a pile diameter of 120 cm. The pile caps of the piers in the broad river bed (P4 ÷ P15) are oblong octagonal (Figure 3a) with 13 piles, a shape which is considered to be beneficial with respect to hydraulics considerations. Pile caps of piers P8 to P15 that may possibly be found in the future in the river bed, are skew with respect to the bridge axis with their short side perpendicular to the river flow. The rest of the pile caps are orthogonal (Figure 3b) with 9 piles arranged at a rectangular 3×3 array.

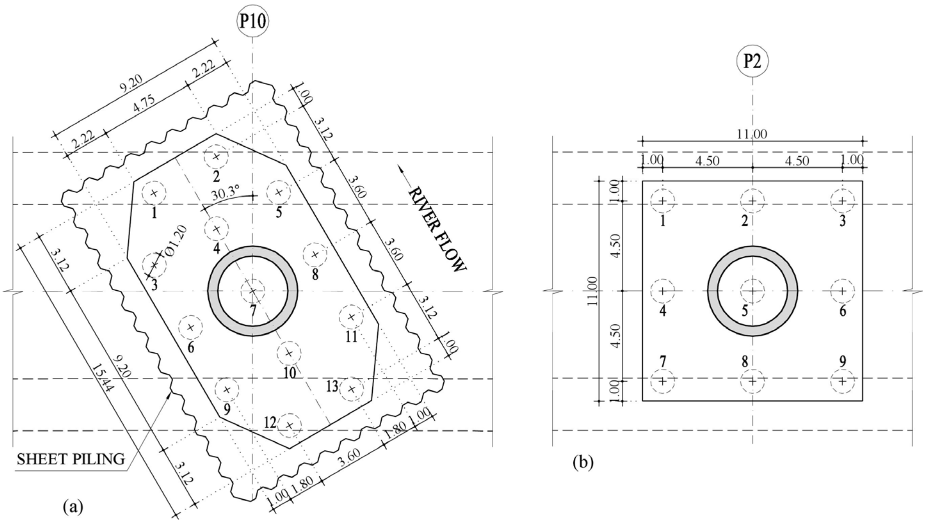

Figure 3: Pile-supported cap footings: (a) Oblong Octagonal; (b) Rectangular

In the river bed area the high water table level, in conjunction with the permeable layers in the bedrock and the continuous river flow, practically prohibit extended and deep excavations due to difficulties in sheet piling, water pumping and the risk of failure due to hydraulic heave. To reduce the necessary excavations and retaining structures, temporary earth fill above the existing ground is utilized as working floor to construct pile caps as high as possible with respect to the ground level. The foundation of all piers that may be found in the river bed is designed so that it can safely carry all bridge loads, service and seismic, even in the case of complete loss of lateral support up to a specified depth due to local erosion/scour, river bed displacement or liquefaction. The above arrangements deal effectively with the problems encountered during the design and construction of the bridge.

Abutment A1 (see Figure 4) is of the seat-type, solid with a height of 7.0m, a backwall with suspended wing walls, and rests on a pile-supported cap footing with 8 Ø100 cm piles. At abutment A2, the steep lateral inclination of the embankment slope (≈2:3) results to an abutment with a height of 16.2 m which is configured as a box-type structure (Fig. 4b) with an intermediate slab at the bearing support level. It rests on a pile-supported cap footing with 16 Ø120 cm piles. A reinforced earth retaining structure is constructed for a length of about 50.0 m behind the abutment up to the portal of the adjacent cut-and-cover structure T13.

The ground is classified as Type B according to the Greek Seismic Code on which Seismic Design of Bridges is based [1] (similar to ground B in Eurocode 8 [2]), which is associated with a design spectrum flat in the range of the corner periods T_1=T_B=0.15 s and T_2=T_C=0.60 s (see Figures 11 and 13 in §4). The viaduct is located in an area of high seismic hazard (Zone II of the Code), with a design ground acceleration of 0.24g, while the importance factor γ_I is equal to 1.30 (importance class III according to Eurocode 8-2, i.e. bridges of critical importance for maintaining communications). Aiming for an elastic design of the seismic isolation system, a behaviour factor q=1.00 is selected.

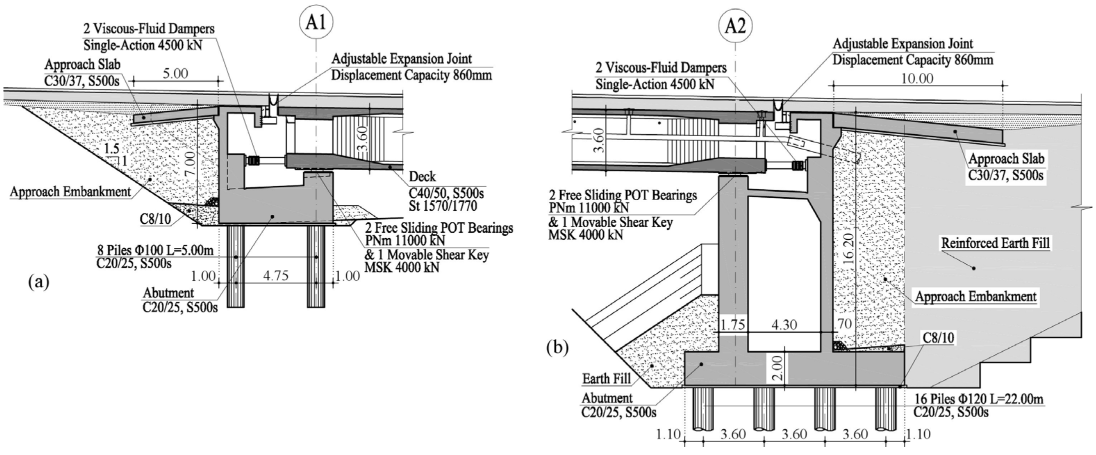
A1
2 Viscous-Fluid Dampers
Single-Action 4500 kN
Approach Slab
C30/37, S500s
5.00
Adjustable Expansion Joint
Displacement Capacity 860mm
3.60
1.5
1
7.00
Approach Embankment
Deck
C40/50, S500s
St 1570/1770
C8/10
2 Free Sliding POT Bearings
PNm 11000 kN
& 1 Movable Shear Key
MSK 4000 kN
8 Piles Φ100 L=5.00m
C20/25, S500s
(a)
1.00
4.75
1.00
Abutment
C20/25, S500s
A2
Adjustable Expansion Joint
Displacement Capacity 860mm
2 Viscous-Fluid Dampers
Single-Action 4500 kN
10.00
3.60
Approach Slab
C30/37, S500s
2 Free Sliding POT Bearings
PNm 11000 kN
& 1 Movable Shear Key
MSK 4000 kN
16.20
Reinforced Earth Fill
Approach Embankment
1.75
4.30
.70
(b)
C8/10
2.00
Earth Fill
Abutment
C20/25, S500s
16 Piles Φ120 L=22.00m
C20/25, S500s
1.10
3.60
3.60
3.60
1.10

Figure 4: Longitudinal sections at (a) Abutment A1 and (b) Abutment A2

3 Seismic Isolation Design

As mentioned earlier, the design seismic action for the bridge is high (design acceleration $\gamma_I \cdot a_g$=0.31g). Moreover, railway bridges are of particular importance, as there is no temporary diversion possibility in case of extensive or even medium damages to the bridge that require closure for repairs; the bridge must be fully functional after the design seismic action retaining its structural integrity and resistance. Furthermore, the high values of dead quasi-permanent and live loads in railway bridges, in conjunction with the relatively tall piers in this viaduct, result in case of an earthquake, in particularly high forces and displacements that have to be kept within acceptable limits. Hence, to reduce the structural response to seismic loading, the bridge is provided with an isolation system. The seismic design of the bridge is based on the Greek “Guidelines for the Design of Seismically Isolated Bridges” [3] and Circular 39/99 “Seismic Design of Bridges” [1]; both documents are largely based on Eurocode 8-Part 2 [2].

Due to the tall and relatively flexible piers, the fundamental period of the bridge was already long and the corresponding value of the design spectral acceleration was consequently low. Therefore, in selecting a proper isolation scheme, the principal aim was to increase the energy dissipated by the structure, and secondly the further lengthening of the fundamental period (period shift effect). Further data that have to be considered when selecting an isolation system (most of them particularly important in the case of railway bridges) are the capability of the isolator units to safely carry all vertical loads, their lateral restoring capability, their elastic stiffness that has to be adequate for service non-seismic horizontal loads (wind, breaking, centrifugal forces) and finally the least possible dependence of their mechanical properties on ageing and temperature factors.

Taking into account all the above aspects, and selecting (as usual) an isolation surface located between the deck and the top of the piers/abutments, the isolation units are arranged as follows (see Figure 5):

- The box girder of the deck rests on each pier by means of two lead-rubber bearings (LRBs) with a vertical load capacity of 22500 kN each. Bearing dimensions are generally 1200×1200/231-200 (mm), where 1200×1200 are the plan dimensions, 231 mm is the total elastomer thickness (Σt_e) and 200 mm is the diameter ($\O_L$) of the lead core, except for P3 and P16 (wherein Σt_e=286, $\O_L$=250). At the outermost, relatively shorter, piers P1, P2 and P17, where the longitudinal displacements due to creep, shrinkage and temperature are high, the bearings are configured as sliding in the longitudinal direction. Plan dimensions are mainly determined by the vertical design load, which is high in railway bridges. Diameter $\O_L$ is selected so that the core is able to (i) resist service horizontal loads with low displacements and without core yielding, and (ii) present adequate damping characteristics for every load cycle. Σt_e is determined by the verification of the maximum permissible shear strain criterion and the avoidance of end slip of the lead plug [4].

- At the abutments the superstructure is supported by means of two pot bearings, movable in both horizontal directions, with a vertical load capacity of 11000 kN. Furthermore, movable shear keys (MSK) with a lateral load capacity of 4000 kN, restrain the transverse differential displacement of the bridge at the expansion joint in order to prevent derailment; it is noted that this important design requirement is generally not applicable in road bridges.

- System damping is further increased by providing two single-acting (in the longitudinal direction) fluid viscous dampers with a load capacity of 4500 kN at each abutment. The selected damping coefficient C of the force-velocity relationship ($F=Cv^{\alpha}$) is 5440 kNs/m and the velocity exponent α=0.15.

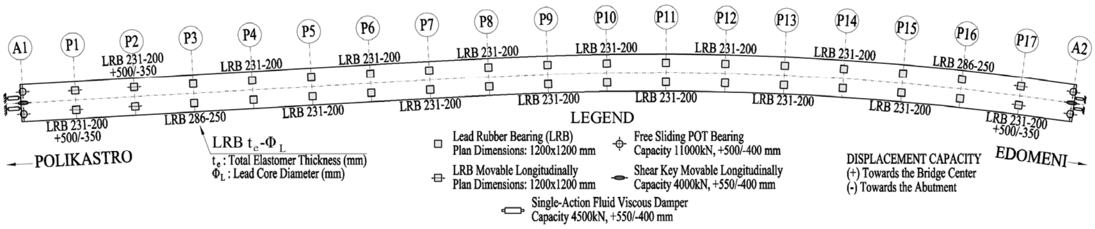
A1
P1
P2
P3
P4
P5
P6
P7
P8
P9
P10
P11
P12
P13
P14
P15
P16
P17
A2
LRB 231-200
+500/-350
LRB 231-200
LRB 231-200
LRB 231-200
LRB 231-200
LRB 231-200
LRB 231-200
LRB 286-250
LRB 231-200
+500/-350
LRB 286-250
LRB 231-200
LRB 231-200
LRB 231-200
LRB 231-200
LRB 231-200
LRB 231-200
LRB 231-200
+500/-350
POLIKASTRO
EDOMENI
LRB t_e-Φ_L
t_e : Total Elastomer Thickness (mm)
Φ_L : Lead Core Diameter (mm)
LEGEND
Lead Rubber Bearing (LRB)
Plan Dimensions: 1200x1200 mm
LRB Movable Longitudinally
Plan Dimensions: 1200x1200 mm
Free Sliding POT Bearing
Capacity 11000kN, +500/-400 mm
Shear Key Movable Longitudinally
Capacity 4000kN, +550/-400 mm
Single-Action Fluid Viscous Damper
Capacity 4500kN, +550/-400 mm
DISPLACEMENT CAPACITY
(+) Towards the Bridge Center
(-) Towards the Abutment

Figure 5: Plan view of Seismic Isolation arrangement

Seismic links (stoppers) in combination with simple elastomeric buffers are provided at the pier heads with an adequate slack for them to remain inactive during the design earthquake in order to ensure structural integrity, while avoiding unseating under extreme seismic displacements (see Figure 6). Seismic links are also arranged as a ‘second line of defence’ at the abutments in combination with the MSK bearings. The minimum overlap length is provided wherever necessary. The expansion joints are of special, non-standardized, design; they are adjustable and accommodate the total seismic design displacement. Rails are interrupted at both abutments.

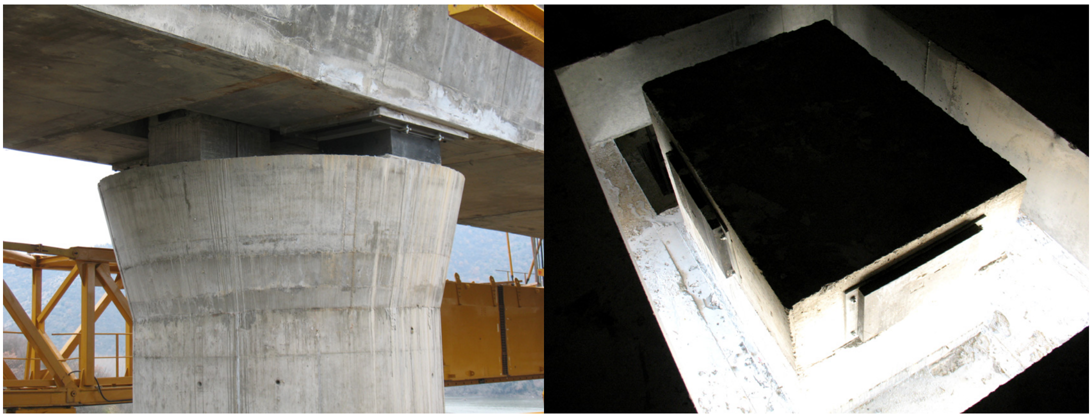

Figure 6: Pier Head and Stopper Details

It is worth mentioning that at the preliminary design phase two more alternatives were investigated prior to selecting the aforementioned solution: (i) an isolated bridge with use of high damping rubber bearings (it was not selected mainly due to concerns regarding the durability of these bearings), and (ii) a semi-integral bridge with 6 of the central piers monolithically connected to the deck (it resulted in a less economical design, particularly with respect to prestressing requirements).

4 Analysis for seismic actions

To verify the performance of the selected passive system, analysis for seismic actions was conducted in three discrete stages of increasing complexity; this is the recommended approach for important design projects, particularly those involving passive systems with dampers. At the preliminary design phase, analysis of the seismic response was carried out utilizing simplified computational models based on the Fundamental Mode (Response) Spectrum Analysis (FMSA). The influence of a number of parameters on the seismic behaviour of the isolated system was investigated. At the next stage a refined 3D finite element model was developed to conduct Multi-mode (Response) Spectrum Analysis (MMSA) of the bridge in three orthogonal directions. System nonlinearities in both FMSA and MMSA are accounted for by means of an iterative procedure. At the final design stage, non-linear response-history analyses (NRHA) were carried out with a view to verifying the results of previous analysis methods and evaluating the performance of the selected isolation system.

4.1 Fundamental mode spectrum analysis

Due to its simplicity the FMSA is a very useful tool for determining the required dynamic characteristics of the system. Considering the superstructure (deck) as a single-degree-of-freedom system and using its effective properties (stiffness, damping, period) one can easily conduct a number of parametric studies to estimate the influence of assumed soil stiffness, flexural cracking of piers, and variability of isolator properties, on the seismic behaviour of the isolated bridge. The rigid deck model was used in the longitudinal direction, while a modified method was used here in the transverse direction where the flexibility of the deck and the substructure has to be taken into account through a simplified multi-degree-of-freedom system.

With regard to the soil stiffness influence, an upper ("stiff") and lower ("flexible") bound is used to take into account the inherent uncertainties when determining the stiffness of the pile-supported cap footing at each pier location, which include variability of lateral and vertical spring stiffness of the piles, shear zone extent in the bedrock layer, and loss of lateral support due to local scour erosion, river bed displacement or liquefaction. The previous "stiff" or "flexible" foundation is combined respectively with a "stiff" or "flexible" value of the effective pier column stiffness which depends mainly on the method and the assumptions used to calculate the moment of inertia subsequent to flexural cracking. 65% ("stiff") and 40% ("flexible") of the moment of inertia of the gross section of the uncracked pier were used in the analysis. Finally the influence of Upper and Lower Bound Design Properties (UBDP and LBDP) of the LRBs calculated according to Annex A of [3] (or Annex J of EC8-2 [2]) was also examined (See Figure 7).

The dampers at the abutments act only in the longitudinal direction. Their stiffness is omitted when calculating the effective stiffness of the system. Their contribution is taken into account through the viscous energy E_{Dvd} dissipated per cycle at the design displacement d_{cd}, which is further added to the hysteretic energy dissipated by the bearings E_{Db}, and the viscous energy dissipated by the substructure E_{Dp} to determine the total dissipated energy per cycle E_D. The effective damping ξ_{eff} of the system can then be calculated in order to estimate a reduced value of the spectral acceleration S_e (T_{eff}, n_{eff}) corresponding to the effective period T_{eff}, with $n_{eff}=n(\xi_{eff})$. The force-displacement behaviour of a single-acting fluid viscous damper is shown in Figure 8.

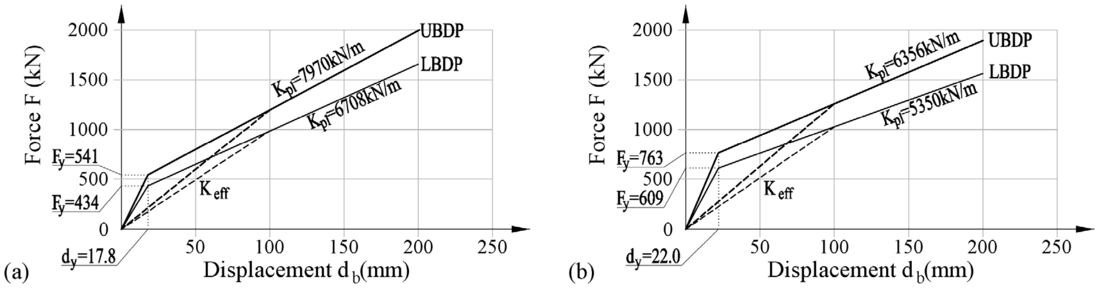

Figure 7: Bounding Design Properties of Lead-Rubber Bearings (a) LRB 1200×1200/231-200 (b) LRB 1200×1200/286-250

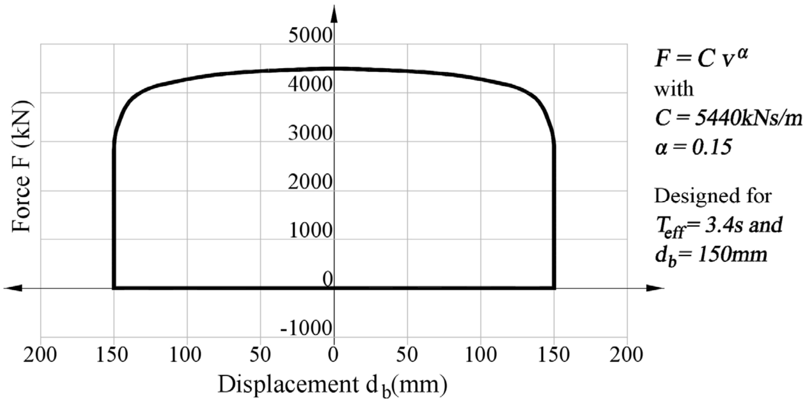

Figure 8: Force-displacement behaviour of a single-acting viscous damper

Results of FMS analysis are presented in Tables 1 and 2. As the results of the d_{cd} values calculated with UBDPs and LBDPs do not differ more than ±15%, multi-mode spectrum and response-history analysis of the next stages may be performed with the LBDPs [2, 3]. The “stiff” substructure assumption, was generally found to be more conservative in relation to the “flexible” one. Spectral acceleration values (S_e/g) and corresponding shear forces were higher by 20 to 25% in the longitudinal and 15 to 25% in the transverse direction. Maximum bearing displacements d_{bd} were also higher by 30÷40% in the longitudinal and 25÷30% in the transverse direction, despite the fact that d_{cd} values were practically equal (difference <2%). As a result the “stiff” substructure assumption in combination with LBDP values for the LRBs was subsequently used at the next analysis stages.

	Bound Design Properties	System Design Displacement d_{cd} (mm)	Max. Bearing Displ. d_{bd} (mm)	Effective Period T_{eff} (s)	ξ_{eff} (%)	S_e / g
“Flexible” Substructure	LBDP	136	68	3.72	42.0	0.039
	UBDP	152	63	3.55	33.0	0.049
“Stiff” Substructure	LBDP	140	89	3.45	40.0	0.047
	UBDP	158	89	3.20	30.0	0.061

Table 1: Fundamental Mode Spectrum Analysis Results (Longitudinal Direction)

	Bound Design Properties	System Design Displacement d_{cd} (mm)	Max. Bearing Displ. d_{bd} (mm)	Effective Period T_{eff} (s)	ξ_{eff} (%)	S_e / g
“Flexible” Substructure	LBDP	354	161	3.67	7.8	0.077
	UBDP	370	131	3.39	6.7	0.094
“Stiff” Substructure	LBDP	348	202	3.36	8.2	0.090
	UBDP	367	170	3.14	6.9	0.116

Table 2: Fundamental Mode Spectrum Analysis Results (Transverse Direction)

4.2 Multi-mode spectrum analysis

A 3D finite element 'stick' model (beam-column elements) was set up in the commercial program SOFiSTiK [5]. Besides the dynamic analysis of the system, the model was also used for all static loading cases. Construction stage loading, as well as service and seismic loads were applied and further combined to design the structure. The model accounted also for longitudinal slope, horizontal alignment, cross section variation, construction joints, prestressing tendon geometry, and effective deck width. Gross (uncracked) stiffness was used for the prestressed concrete deck, while its torsional stiffness was reduced by 50% assuming minor cracking. Separate models comprising 2D and beam elements were constructed for the pile-supported cap footings of every pier, which were further used to calculate the upper and lower bound values of the spring stiffness matrix at the bottom of the piers. The stiffness of the bearings in the horizontal direction depends on the rate of loading due to creep phenomena and is duly calculated for service loads.

As mentioned previously, 65% of the moment of inertia of the gross section of the uncracked pier ("stiff" assumption) was used for the equivalent modal analysis. System nonlinearities were accounted for by means of an iterative procedure, similar to that of the FMSA, where secant stiffness of isolators, effective damping, and ordinates of the design spectrum are recalculated at each iteration based on the displacements of the previous step until convergence criteria are satisfied. The first two significant modes calculated according to the above approach are shown in Figures 9 and 10. The results are in very good agreement with the FMSA. The modified elastic response spectrum used in the analysis for the two horizontal directions (X and Y) is shown in Figure 11. The damping correction factor n_{eff} $(=[0.10/(0.05+\xi_{eff})]^{0.5})$ is applied to modes having periods higher than $0.8T_{eff}$. The vertical component of the seismic action is 70% of the horizontal one [2, 3].

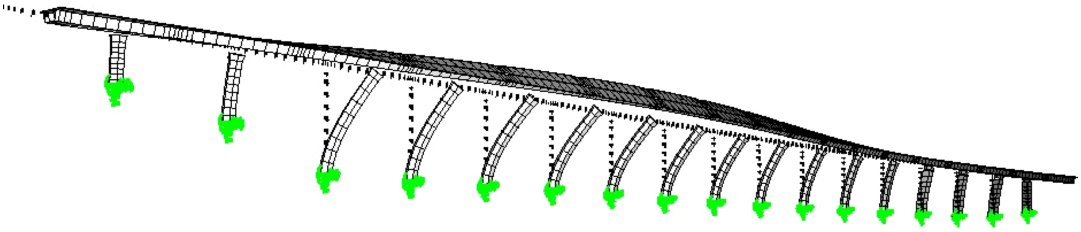

Figure 9: Longitudinal Mode, $T_{x,eff}$=3.45s, ξ_{eff}=39.5%, d_{cd}=0.14m

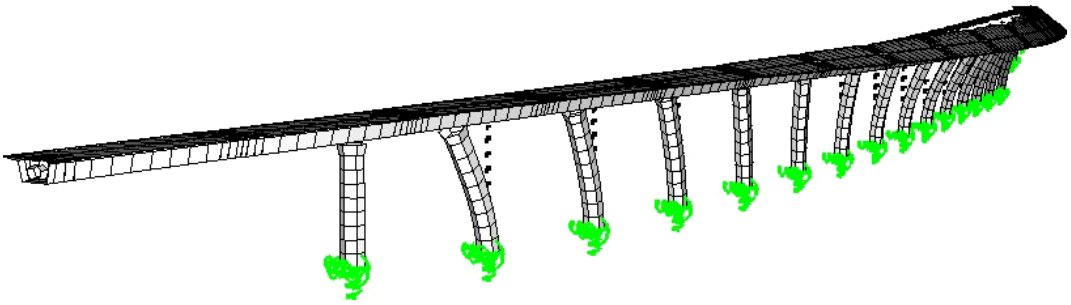

Figure 10: Transverse Mode, $T_{y,eff}$=3.47s, ξ_{eff}=8.1%, d_{cd}=0.28m

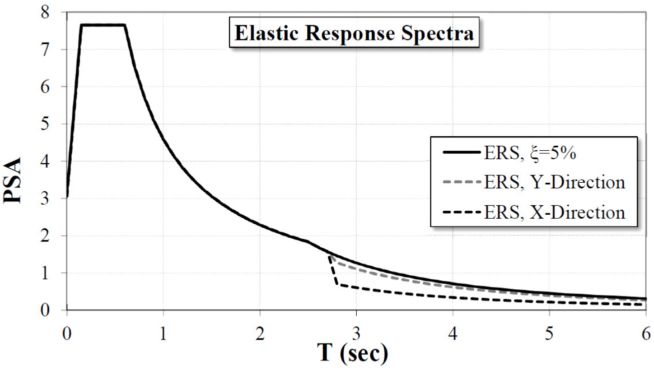

Figure 11: Horizontal components of Response Spectra used in the analysis

4.3 Non-linear response-history analysis

At a final design stage, non-linear response-history analyses (NRHA) were carried out using SAP2000 v.10 [6] to verify the results of previous analysis methods and evaluate the performance of the selected isolation system. Elastic modal analysis results were compared with those from SOFiSTiK for verification. For the inelastic analyses, nonlinear properties are only assigned to isolators where the input energy is dissipated (LRBs, Dampers), while the rest of the structure is assumed to remain elastic (q=1.0, ξ=5%). LRBs exhibit hysteretic behaviour (see Figure 12) and the Nonlinear link "Rubber Isolator" is used. Double-action viscous Dampers (Maxwell model) are combined with a Nonlinear Gap element in series in order to account for the single-acting behaviour (see Figure 8).

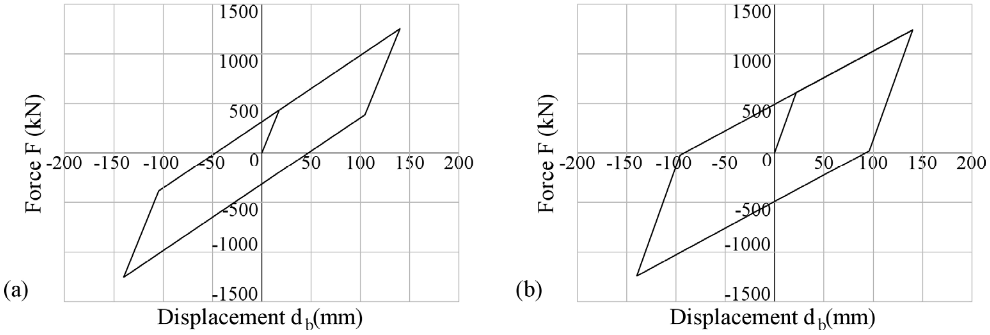

Figure 12: Simplified bilinear hysteresis loops of LRBs at the design displacement (a) LRB 1200×1200/231-200 (b) LRB 1200×1200/286-250

The suite of accelerograms required for response-history analysis was compiled using the basic criteria adopted by modern codes like Eurocode 8; for minimising the uncertainty associated with the choice of seismic input, both artificial and natural records were included, as follows: Three pairs of natural records (shown unscaled in Figure 13), were selected from the European Strong Motion Database [7] taking into account the seismogenetic features of the sources and the soil conditions appropriate to the site of the bridge; more specifically, the ground motions from which the records originated fell within the narrow range Ms=6.0÷6.5, R=5÷25 km resulting from de-aggregation of seismic hazard in the area of the bridge. All records were scaled to the design seismic intensity as described in the following paragraph. In addition, seven synthetic accelerograms compatible with the design spectrum, generated using the program ASING [8] were included in the suite. The average of the individual responses may be used as the design value of the action effects, as non-linear dynamic analysis is performed with more than seven independent pairs of horizontal ground motions [2, 3]. Both direct time integration (Hilber–Hughes–Taylor, HHT) and mode superposition algorithms (Fast Nonlinear Analysis, FNA) were used, and results were cross-checked.

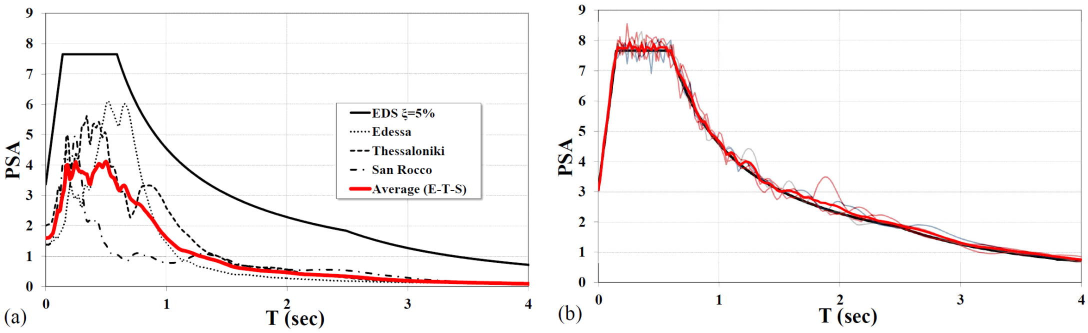

Figure 13: Spectra of (a) natural and (b) synthetic records

Appropriate assumptions had to be made for issues still not fully covered by code provisions, such as combination rules in different directions in which records are applied, and scaling of natural records [9]. Response-history analyses were conducted with 100% of one horizontal synthetic record acting simultaneously with 30% of the other one (and 30% vertically). To derive a realistic value for the scaling factor to be applied to the natural records, the pertinent procedure of [3] was used (SRSS spectra used to derive an average ensemble spectrum), which is similar to that of EC8-2, assuming however that the "*not lower than 1.3 times the 5%-damped elastic response spectrum of the design seismic action, in the period range between* $0.2T_1$ *and* $1.5T_1$" requirement is not applied to the ordinates of the spectra, but rather to the area under them. A scaling factor of 5.3 is thus obtained, instead of values close to 10.0 which are deemed to be unrealistic. Of course, in the last few years even more sophisticated procedures for selection and scaling of natural records have been suggested by various researchers (e.g. [10]), based on similarity of the spectra rather than on the (M, R) range, but at the time of the design of the bridge they were still at a relatively early stage of development (this is still an issue of current research) and in any case they require use of specific software that was not available at the time.

Indicative results of displacements, force-displacement diagrams of non-linear elements, and comparisons between NRHA and results obtained by MMSA are presented in Figures 14 to 17. As mentioned above, average maximum (absolute) values were used for NRHA verifications.

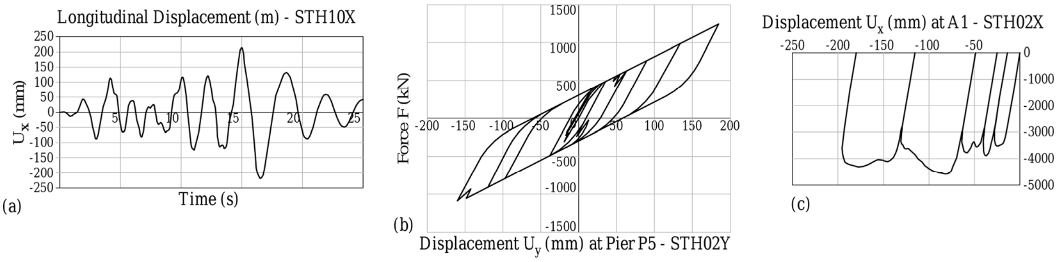

Figure 14: Indicative results from NRHA for (a) Longitudinal displacement d_{cd}, (b) LRB F-d diagram and (c) Damper F-d diagram

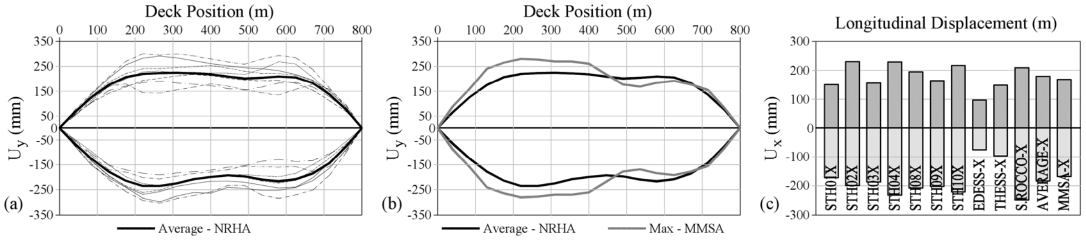

Figure 15: (a) Transverse Displacements for NRHA and (b) Comparison with MMSA results, (c) Longitudinal Displacement for NRHA-MMSA

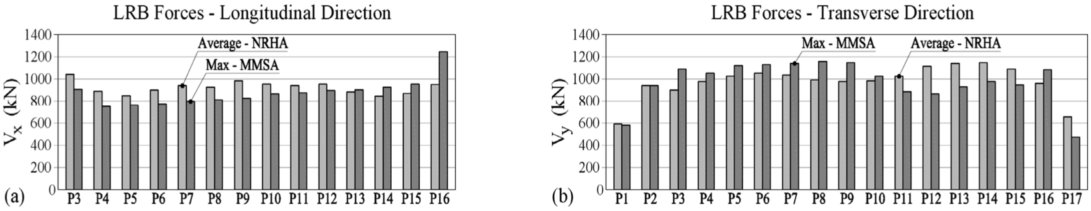

Figure 16: LRB force comparison between NRHA and MMSA: (a) Longitudinal direction and (b) Transverse direction.

As can be seen in Figures 15 to 17, the results are generally found to be in good agreement between equivalent elastic and inelastic analyses. In the longitudinal direction deck displacements are about 14 cm, similar for both methods. In the transverse direction results of NRHA tend to be more uniformly distributed among the piers, with the maximum average displacement (≈25 cm) not differing much from that of the MMSA (≈28 cm). There is a rather noticeable difference, though, in the shape of the elastic displacement profile of the deck between the two methods, i.e. the NRHA predicts a smoother profile than that resulting from the mode superposition carried out in the MMSA. This issue however is not considered as major, as the equivalent elastic method gives slightly larger maximum displacement than the more refined NRHA.

With regard to shear forces in the LRBs, up to 15% higher longitudinal forces are predicted by NLRH for piers P3 to P12 (for the other piers MMSA is more conservative than NRHA), and up to 29% higher transverse forces are predicted for piers P11 to P15. Moreover, slightly higher bending moments are predicted for piers

P12 to P14. Overall, there is no distinct tendency of either method (equivalent elastic and inelastic) to over- or under-predict a certain response quantity; the most notable discrepancy is in the distribution of forces and displacements along the length of the bridge, attributed mainly to the low frequency content of the synthetic records (resulting from the requirement to match the design spectrum), which enhances the participation of lower pier column modes to the response.

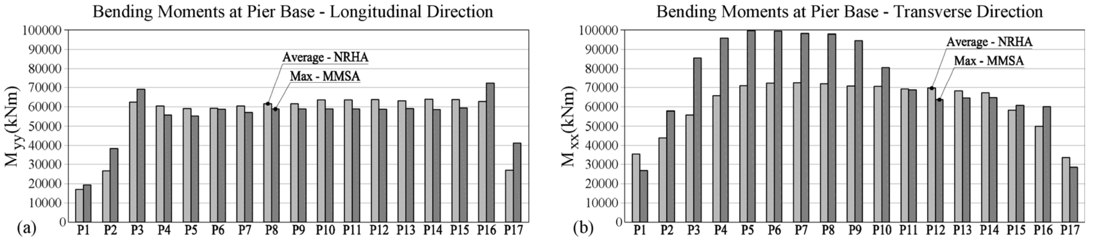

Figure 17: Pier Base bending moment comparison between NRHA and MMSA (a) Longitudinal direction and (b) Transverse direction

As a rule, synthetic records were found to produce fatter and more symmetric hysteresis loops in the LRBs, attributed to the larger number of acceleration peaks (values close to the PGA), in comparison to the natural records.

4.4 Final evaluation of the passive system

The proposed passive system of isolators and dampers made it possible to keep seismic forces and displacements of the bridge within acceptable limits. The seismic energy dissipation capacity of the proposed system, as well as the verification of all members designed, were confirmed with the use of inelastic analyses; more specifically:

- In the longitudinal direction, where viscous (velocity dependent) and hysteretic (displacement dependent) isolators cooperate, and wherein the fundamental mode dominates the response, displacements and accelerations are substantially reduced. A particularly high effective damping close to 40% was attained and the calculated seismic displacement of the deck was 140 mm.

- Available reserves in the shear deformation capacity of the bearings were sufficient to accommodate some local increases (with respect to the elastic design) in LRB forces.

- The minimum reinforcement ratio of 1.25%, provided at the base of the piers according to Priestley’s recommendation [11] for hollow circular sections, resulted in sufficient reserve capacity of the pier columns to safely accommodate the slightly higher forces predicted by the NRHA for some piers.

Furthermore, the selected system exhibits adequate vertical load carrying capacity, self-restoring capability, and sufficient elastic stiffness under non-seismic service horizontal actions such as braking/acceleration, wind and centrifugal loads.

5 Conclusions

The design of the major railway bridge presented herein can be deemed as a paradigm of the challenges the designer faces whenever such a bridge has to be built in a high seismic hazard area. Notably, displacement control, which is an issue in all cases, is even more difficult to achieve in the case of railway bridges wherein stricter requirements apply. In the longitudinal direction of the bridge a particularly high supplemental damping (around 40%) had to be provided (through a combination of LRBs and viscous fluid dampers), while in the transverse direction, the detailing of the isolation system had to be such as to restrain displacements at the abutments where the only expansion joints were located. Moreover, the high vertical loads typical in this type of bridge render it necessary to provide isolators (bearings) that are not only dissipative, but also strong enough to resist high axial loads.

Due to the rather complex, and certainly nonlinear under the design seismic action, behaviour of the passive systems such as that presented herein, advanced analysis tools (NRHA) have to be used in verifying the design, which, inevitably (in a practical context), is based on equivalent elastic analysis. Besides difficulties in the modelling of the structure, the selection of the input accelerograms to be used in dynamic response-history analysis, including the issue of scaling natural records that are the preferred choice (artificial records are characterised by unrealistic frequency content) is a critical issue, as inappropriate choices might lead to over-conservatism in the design of the structure (this is not uncommon, in the experience of the authors). Furthermore, the substantial variability in the response to different records, seems to justify the choice made here to provide enough reserve ductility to the piers through careful detailing of the reinforcement, despite the use of elastic design (q=1.0).

Acknowledgements

The design of the T12 railway bridge was carried out in 2006 by the consulting firm METE SYSM S.A. for the project owner ERGA OSE S.A. The bridge was constructed by MICHANIKI S.A. The first author was the expert consultant for the seismic isolation design. The authors wish to thank Prof. A. Sextos from the Aristotle University of Thessaloniki for providing the artificial records that formed part of the suite used in this study, and Dr D. Koutsoukos from ERGA OSE S.A. for the valuable exchanges of opinion on several aspects of the design of the bridge.

References

[1] Greek Ministry for Environment, Planning and Public Works, Directorate for the Design of Road Works, "Seismic Design of Bridges", Circular 39/99, Athens, 1999.

[2] CEN Techn. Comm. 250 / SC8 "Eurocode 8: Design of structures for earthquake resistance - Part 2: Bridges (EN 1998-2)", CEN, Brussels, 2005.

[3] Greek Ministry for Environment, Planning and Public Works, Directorate for the Design of Road Works, "Guidelines for the Design of Seismically Isolated Bridges", Athens, 2004.

[4] R.I. Skinner, W.H. Robinson, G.H. McVerry, "An Introduction to Seismic Isolation", John Wiley & Sons, 1993.

[5] SOFiSTiK GmbH, SOFiSTiK v.99: Structural Analysis and Design Program, München, Deutschland, 2005.

[6] Computers and Structures Inc., SAP2000 v.10: Three dimensional static and dynamic finite element analysis and design of structures, Berkeley, California, 2004.

[7] N. Ambraseys, P. Smit, R. Berardi, D. Rinaldis, F. Cotton, C. Berge: Dissemination of European Strong-Motion Data. CD-ROM collection, European Commission, DGXII, Science, Research and Development, Bruxelles, Belgium 2000.

[8] A. Sextos, K. Pitilakis, A.J. Kappos, "Inelastic dynamic analysis of RC bridges accounting for spatial variability of ground motion, site effects and soil-structure interaction phenomena. Part 1: Methodology and analytical tools", Earthquake Engineering and Structural Dynamics, 32 (4), 602-327, 2003.

[9] A.J. Kappos, E. Dimitrakopoulos, "Analysis and Assessment of a Seismically Isolated Bridge", Earthquake Resistant Engineering Structures V (ERES 2005), WIT Press, 625-635, 2005.

[10] E.I. Katsanos and A.G. Sextos, "ISSARS: An integrated software environment for structure-specific earthquake ground motion selection", *Advances in Engineering Software*, 58, 70-85, 2013.

[11] M.J.N. Priestley, "Seismic design issues for hollow bridge piers", Report prepared for EGNATIA ODOS AE, Thessaloniki, Greece, 1998.